I.J. Wireless and Microwave Technologies, **2023, 5, 34-47**
Published Online on October 8, 2023 by MECS Press (http://www.mecs-press.org/)
DOI: 10.5815/ijwmt.2023.05.04

Design of 28/38-GHz Dual-Band Millimeter Wave Antenna based on SIW for Future Cellular Communication Systems

Khaled A. M. Al Soufy*
Department of Electrical Engineering, Ibb University, Ibb City, Yemen
E-mail: kalsoufi@ibbuniv.edu.ye
ORCID iD: https://orcid.org/0000-0002-1224-1405
*Corresponding Author

Nagi H. Al-Ashwal
Department of Electrical Engineering, Ibb University, Ibb City, Yemen
E-mail: nlashwal@yahoo.com
ORCID iD: https://orcid.org/0009-0005-9566-1956

Faisal S. Al-Kamali
Department of Electrical Engineering, Ibb University, Ibb City, Yemen
E-mail: faisalalkamali@yahoo.com
ORCID iD: https://orcid.org/0000-0001-7086-6684

Redhwan Saad
Department of Electrical Engineering, Ibb University, Ibb City, Yemen
E-mail: alnakhlany@gmail.com
ORCID iD: https://orcid.org/0000-0001-7241-9327

Majed A. AL-Sayadi
Department of Electrical Engineering, Ibb University, Ibb City, Yemen
E-mail: Alsayadimajed@gmail.com

Received: 16 January, 2023; Revised: 03 March, 2023; Accepted: 20 May, 2023; Published: 08 October, 2023

Abstract: The millimeter wave (mmWave) band has gained significant attention due to its potential to cater to the rapidly increasing wireless data rates. Due to the reduced wavelength in mmWave communications, it is possible to implement large antenna arrays at both the transmitter and the receiver. Designing small antennas in the mmWave range presents many challenges, which is the main aim of this paper. The aim of this work is to proposed an efficient design of a dual-band mmWave antenna, with the dimension of 26.5mm×7.0mm×0.254mm, for future cellular communication systems using a substrate integrated waveguide (SIW). The elements of the proposed antenna consist of SIW cavity with one longer longitudinal slot and another shorter engraved slot in one of the conducting planes (1×2) for 28 GHz and 38 GHz, respectively. The substrate duroid 5880/Rogers are used with a loss tangent and dielectric constant of 0.003 and 2.2, respectively. The CST Microwave Studio, an industry-standard software, was utilized to conduct the simulation results. The proposed antenna's performance was evaluated by analyzing its gain, radiation pattern, and return loss at the frequencies of 28 GHz and 38 GHz. Furthermore, it is compared with other relative works. The single antenna element was able to attain an impedance bandwidth (S11< -10 dB) of 1.32 GHz and 3.1 GHz, with a satisfactory gain of 6.1 dBi and 5.81 dBi at 28 GHz and 38 GHz, respectively. The results indicate that the designed antenna can attain consistent and adjustable dual-frequency performance, making it a viable option for future cellular communication systems.

Index Terms: mmWave, radiation pattern, return loss, and gain

1. Introduction

The demand for high data-rate applications has driven the evolution of wireless communications. The applications of the fifth generation (5G) require higher bandwidths for higher data rates, which in turn have led to the use of millimeter wave (mmWave) bands. Recently, the 3rd Generation Partnership Project (3GPP) has standardized the 28 GHz and 38 GHz mmWave bands [1]. Moreover, The Federal Communication Commission (FCC) has allocated both 28 GHz and 38 GHz mmWave bands for 5G communication networks [2]. In China, for instance, 28 GHz and 38 GHz mmWave bands have been dedicated for 5G [3]. System operating in the mmWave bands suffers from high path loss and high penetration loss. In addition, it is crucial for mmWave 5G base stations to have a compact and lightweight design. Hence, the antenna must possess low return loss and high gain while occupying minimal space. New antennas structure such as metamaterial, microstrip antennas and substrate integrated waveguide (SIW) have been introduced to meet these demands. SIW has been developed by K. Wu [3]. There are various types of SIW antennas [4], such as cavity-backed antenna, slotted SIW antenna, antipodal tapered slot antenna, dielectric resonator antenna, etc. SIW has has garnered significant attention by researchers due its desirable features such as light weight, high power capacity, high selectivity, high-factor, low profile, etc. The use of SIW for antenna design for the mmWve is very promising. Recently, there has been much research on SIW technology. Most of the relevant previous studies have mentioned that SIW is a suitable choice at mm-Wave frequencies when compared with conventional printed circuits and waveguides counterparts [5-12]. In [13], a dual-band slotted SIW four-element array antenna was designed to achieve high efficiency and gain. This antenna array operated at frequency bands of 28 GHz and 38 GHz. It was designed based on duroid 5880/Rogers substrate which has loss dielectric constant and tangent of 2.2 and 0.003, respectively. In [14], the authors have proposed a single (1x2) slotted-SIW dual-band antenna at 28GHz and 38 GHz. For single antenna, the obtained impedance bandwidth was 0.45 GHz and 2.20 for 28GHz and 38 GHz respectively. In addition, the maximum gain of 5.2 dBi for 28 GHz and 5.9 dBi for 38 GHz. To achieve a high gain, a linear array consisting of four elements (1x4) was also designed, which attained a maximum gain of 11.9 dBi and 11.2 dBi at 28 GHz and 38 GHz, respectively. The authors in [15] proposed an 8×8 cavity-backed slot array antenna for enhancing the bandwidth in fixed beam applications. A modified bow-tie cavity slot was used instead of the conventional rectangular cavity slot. In [8], a 1×4 SIW dual-band antenna array topology has been designed for operating in the 28GHz and 38 GHz frequency bands. Four miniaturized quarter-modes of SIWs have been adopted to support the designed antenna with four distinct resonance frequencies. In [16], a dual-polarized subarray antenna that operates at 28/38 GHz dual-band for 5G generation was presented. The unit element was designed to operate at 27.6-30.8 GHz and 35.4-38.9 GHz with gain of 6.9 dBi and 5.3 dBi at 28 GHz and 38 GHz respectively. The 2×2 subarray with 4 vertical and 4 horizontal feeding ports and a design an array area of 34×36 mm2 using antenna elements of 2.5mm long have been used. The 2×2 subarray with 4 horizontal and 4 vertical feeding ports and a design an array area of 34×36 mm^2 using antenna elements of 2.5mm long have been used. At 28 GHz and 38 GHz, the designed antenna system was able to achieve a high gain of 13.1 dBi and 13.2 dBi, respectively. However, that gain incurs the high cost of antenna array volume. The authors in [17] proposed proposed a novel SIW antenna with stepped long slots, which operates in dual-port and dual-band frequencies (28/38 GHz), specifically intended for 5G base stations. In [18], a SIW antenna has been designed to operate at dual band of 28 GHz and 38 GHz for 5G cellular network applications. The obtained gains were 7.05 dBi and 8.32 dBi at 28 GHz and 38 GHz respectively. The proposed antenna achieves bandwidth of 0.982 GHz and 0.354GHz for 28 GHz and 38 GHz respectively.

In this paper, we propose the design of a (28/38) GHz dual-band SIW slot antenna for use in future mobile communication networks. The main objective and contribution of this work is that the parameters of the proposed antenna, including length and width of each slot and its positions, are tuned through three steps until the acceptable characteristics are obtained for use in future cellular communication systems. In the first step, a single band slotted SIW Antenna at 38 GHz is designed. In the second step, the antenna designed in the first step will be modified to be used for a 28 GHz band. In the last step, the antenna design in the previous two steps will be modified in such a way to be used for dual bands (28 and 38 GHz). The designed waveguide slots antenna offers several advantages such as a straightforward design and fabrication process, linear polarization, low loss, low cross-polarization, and high gain and power handling capacity. so it can be used in the future cellular communication systems. Compared to all the previously mentioned existing works, the proposed antenna design demonstrates significantly better performance in terms of gain, return loss, and radiation pattern. The rest of this paper is set up as follows. Section 2 presents the theoretical design of SIW slots antenna. Section 3 presents the results and discussion. Section 4 compares between this work and the other relevant works. Section 5 concludes the paper.

2. SIW Slots Antenna

SIW is essentially an integrated version of the conventional metallic rectangular waveguide. It involves a dielectric substrate attached to its lower part, with metal layers on both the top and bottom surfaces. The waveguide wall is defined by metal vias within the substrate. The main advantages of SIW antenna structure are simplicity of design, complete shielding, and low losses. Furthermore, SIW structures can be integrated with various active devices and microwave monolithic integrated circuits, as well as microstrip lines and coplanar waveguides. In addition to its thickness $\boldsymbol{h}$ and relative permittivity $\boldsymbol{\varepsilon_r}$, an SIW also has three other important parameters, which include the width $\boldsymbol{a}$ of the waveguide, the diameter $\boldsymbol{d}$ of the metalized via, and the distance $\boldsymbol{p}$ between adjacent metalized vias. These parameters are illustrated in Fig.1. Within a given waveguide, it is possible to propagate several modes of electromagnetic waves as shown in Fig. 2. The cutoff frequency for each mode can be determined by the physical dimensions of a waveguide.

Transverse Electric (TE_{10}) is the dominant mode in rectangular waveguide because it has the lowest cutoff frequency (f_c) and the highest cutoff wavelength ($\boldsymbol{\lambda_C=2a}$) out of all the TE_{mn}. Generally, the cut-off frequency of modes TE_{m0} can be derived using [19]:

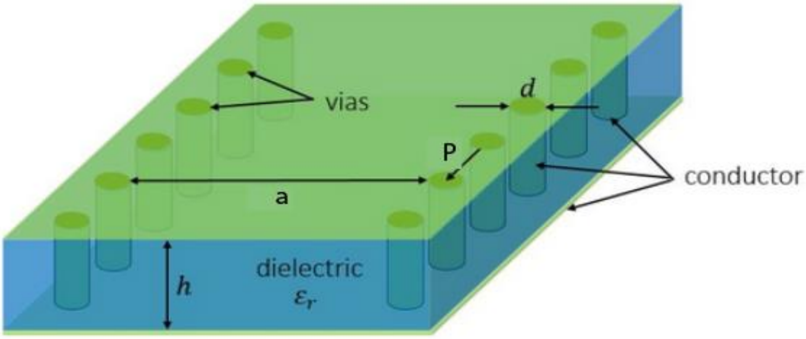

Fig. 1. Configuration of an SIW.

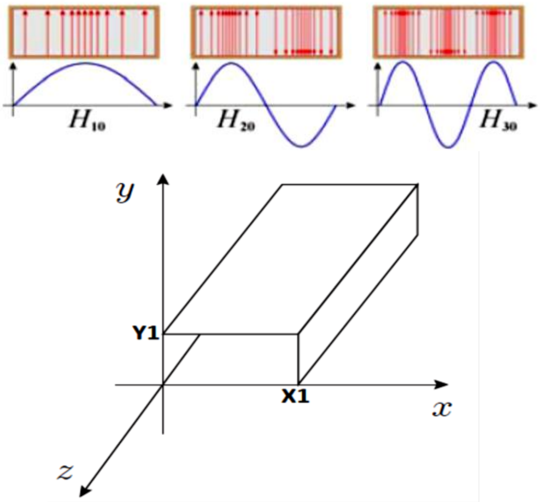

Fig. 2. Several modes of electromagnetic waves

$$f_{c_{mn}} = \frac{c}{2\pi\sqrt{\mu\varepsilon}}\sqrt{\left(\frac{m\pi}{a}\right)^2 + \left(\frac{n\pi}{b}\right)^2} \tag{1}$$

if m=1 and n=0, it means $f_{c_{10}}$, then

$$f_{c_{10}} = \frac{c}{2\pi\sqrt{\mu\varepsilon}}\left(\frac{m\pi}{a}\right) = \frac{cm}{2\pi a\sqrt{\mu\varepsilon}} \tag{2}$$

where $\boldsymbol{m}$ is the mode number, $\boldsymbol{a}$ is the equivalent width, $\boldsymbol{\mu}$ is the permeability and $\boldsymbol{\varepsilon}$ is the permittivity. Consequently, the corresponding guided wavelength can be determined by:

$$\lambda_g = \frac{\lambda_0}{\sqrt{\varepsilon_r\left(1-\left(\frac{f_c}{f}\right)^2\right)}} \tag{3}$$

Where $\boldsymbol{\lambda_0}$ is the free space wavelength, $\boldsymbol{f_c}$ is the cutoff frequency and $\boldsymbol{\varepsilon_r}$ is the dielectric constant of waveguide. $\boldsymbol{a_e}$ can be calculated by:

$$w = a_e = a - \frac{d^2}{0.95\,p} \tag{4}$$

Where $\boldsymbol{d}$ and $\boldsymbol{p}$ are physical parameters of via-holes as shown in Fig. 1. Once $\boldsymbol{a_e}$ is computed the obtained dielectric-filled rectangular waveguide will have the same cut-off frequency of TE_{10}.

One of the primary challenges in the design of SIWs is the presence of electromagnetic bandgaps, which can cause stopband effects that disrupt the signal transmission. To ensure the optimal functioning of an SIW, it is crucial to prevent the occurrence of bandgaps within the waveguide's bandwidth. As mentioned in [4], there is a region of SIW structure at which the bandgap is not present. This region can be given by:

$$0.05 < \frac{p}{\lambda_c} < 0.25 \tag{5}$$

2.1. Loss Considerations

Energy loss in transmission can occur due to various physical mechanisms such as radiation leakage, conductor loss, and dielectric loss. The suitable selection of dielectric material and conductor type can mitigate the losses incurred by the first and the second mechanisms respectively. However, the gaps between the slots and the metalized vias lead to the radiation leakage which can be given by:

$$\alpha_R = \frac{\frac{1}{a}\left(\frac{d}{a}\right)^{2.84}\left(\frac{p}{d}-1\right)^{6.28}}{4.85\sqrt{\left(\frac{2a}{\lambda_g}\right)^2-1}} \quad \left[\frac{dB}{m}\right] \tag{6}$$

Where $\boldsymbol{\alpha_R}$ is the radiation leakage. From equation (4), the radiation leakage depends heavily on $\boldsymbol{p}$ and $\boldsymbol{d}$ parameters. Thus, leakage loss can be reduced. It is noted that to reduce the leakage losses, the hole diameter $\boldsymbol{d}$ should satisfy the geometric condition of $\boldsymbol{d<\lambda_g/5}$ [19].

3. Antenna Design and Results analysis

Most of the antennas of 28/38 GHz bands are designed by using either multilayer technology, which is complicated and difficult to manufacture or a very thick substrate (more than 1 mm) which results in spurious radiations. In this work, the second case with a small thickness is adopted to select substrate and design techniques where the use of a substrate at this thickness can improve the impedance bandwidth as well as provide adequate strength to support the structure and avoid surface wave as well. The substrate material of Rogers RT/duroid 5880 is utilized to design the antenna with substrate thickness (0.254 mm) and copper cladding layer thickness ($\boldsymbol{h_{PEC}}$)17.5μmm. The metal used for via holes metallization and cladding is copper with conductivity $\sigma = 5.8\times10^7$ s/m. Furthermore, the antenna design incorporates a tapered microstrip line transition to achieve a wide bandwidth. The design work has been carried out using computer simulation technology (CST) Microwave Studio [20]. To achieve the research objectives, the antenna design is performed through the following three steps:

- Step (I): Single Band slotted SIW Antenna at 38 GHz is designed.
- Step (II): The designed antenna in step (I) will be modified to be used for a 28 GHz band.
- Step (III): The design of antenna in the previous two steps will be modified in such a way to be used for dual bands (28 and 38 GHz).

3.1. Step(I): Design of Single Band slotted SIW Antenna at 38 GHz

The proposed antenna is displayed in Fig. 3. The SIW has coupling slots that are cut on its top surface. The proposed SIW slotted antenna has longitudinal slots in the upper metallic layer of the waveguide, i.e., parallel to the length of the guide. As depicted in Fig. 3, the longitudinal top wall slot of the SIW operates as a resonant mode with a resonant length of approximately $\lambda_g/2$. The short circuit is located approximately $\lambda_g/4$ or $3\lambda_g/4$ away from the center of the closest slot, denoted as Y_{slot}. These longitudinal top wall slots are designed to cut transverse shunt currents. For 38 GHz single band operation, the lengths and widths of the first and second slots are: 4.5 mm and 0.17 mm respectively. In order to maintain reasonably low radiation losses, the separation between diameter of vias and vias are selected to be 0.5 mm and 1 mm respectively. Antenna reflection coefficient before enhancement is shown in Fig. 4. The overall antenna dimensions are $26.5\times7.0\times0.254\text{mm}^3$. In order for the H-plane sectoral SIW slotted antenna to be excited in a single mode, the width $\boldsymbol{a}$ of the feeding waveguide (as shown in Fig. 4) must satisfy the condition: $\boldsymbol{\lambda_0/(2\sqrt{\varepsilon_r}) \leqslant a \leqslant \lambda_0/\varepsilon_r}$). In addition, the height $\boldsymbol{h}$ should satisfy the condition of $\boldsymbol{h \leqslant \lambda_0/(2\sqrt{\varepsilon_r})}$ where $\boldsymbol{\lambda_0}$ is a wavelength in free space. So that, for only exciting the fundamental mode TE_{10}, $\boldsymbol{h}$ must be 0.254mm. On the other hand, if the substrate thickness is decreased (more thinner), the mismatch between the antenna slots and the air increases, resulting in a shift in the center frequency of the antenna, as depicted in Fig. 5. The optimized designed parameters values after tuning are listed in Table 1. Fig. 6 shows the return loss |S11| of the designed SIW slot antenna from 25 GHz to 40 GHz.

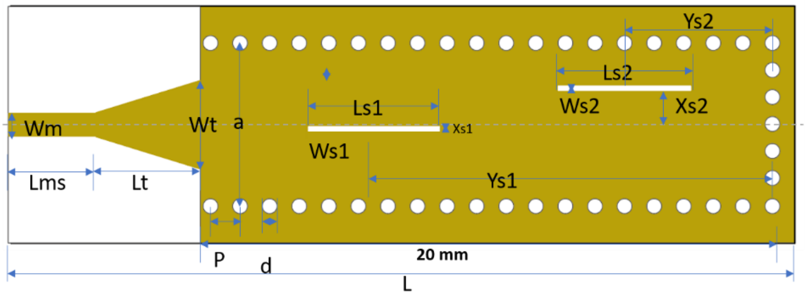

Fig. 3. SIW Dual-Slots at 38 GHz.

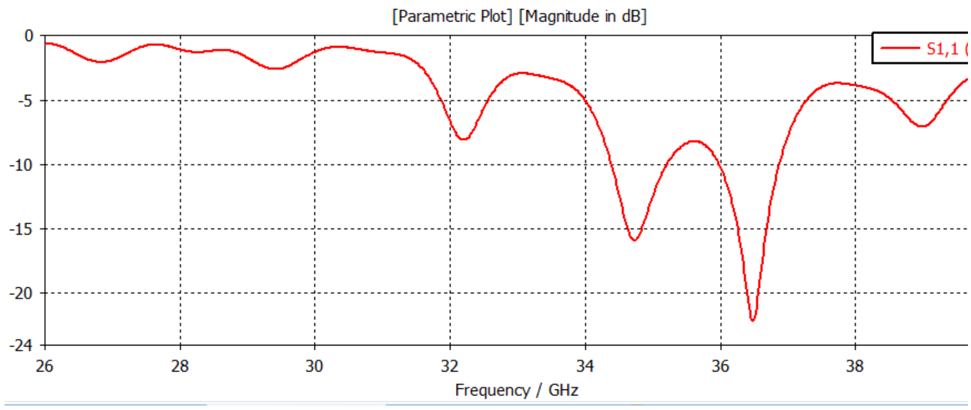

Fig. 4. Antenna Reflection Coefficient before enhancement.

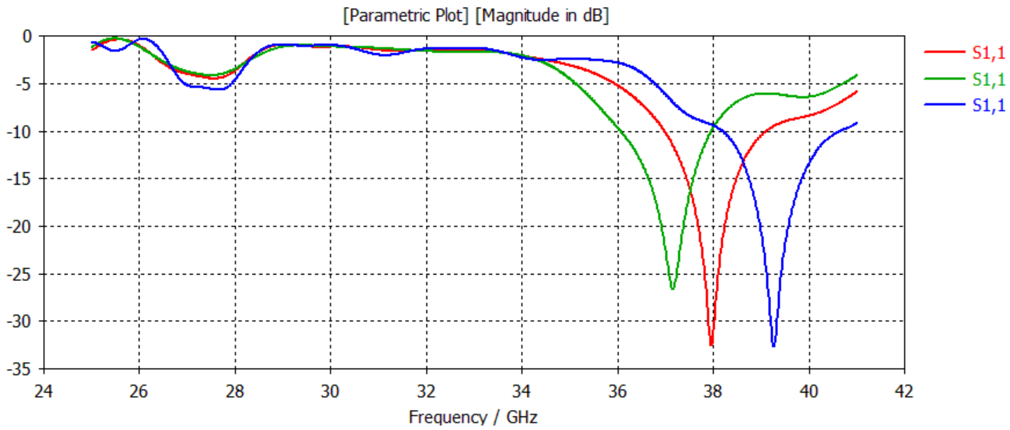

Fig. 5. Comparison of antenna reflection coefficient |S11| at different substrate thickness h =0.127, 0.254, 0.381.

Table 1. Antenna design parameters at 38GHz, Step(I)

Symbol	Value(mm)	Description
W	7	Antenna width
L	26.5	Antenna length
P	1	Center-to-center via holes Separation
D	0.5	Via holes diameter
A	5.5	Waveguide width
L_{s1}	4.5	Length of slot1
H	0.254	Substrate thickness
h_{pec}	0.0175	Metal thickness
L_{s2}	4.5	Length of slot2
W_{s1}	0.17	Width of slot1
W_{s2}	0.17	Width o slot2
W_t	3	Tapered Transition width
L_t	3.5	Tapered Transition length
W_m	0.789	50 Ω feed line width
X_{s1}	0.06	Position of slot1 at X-axis
X_{s2}	-1.15	Position of slot2 at X-axis
L_{ms}	3	50 Ω feed line length
Y_{s1}	13.7	Position of slot1 at Y-axis
Y_{s2}	5	Position of slot2 at Y-axis

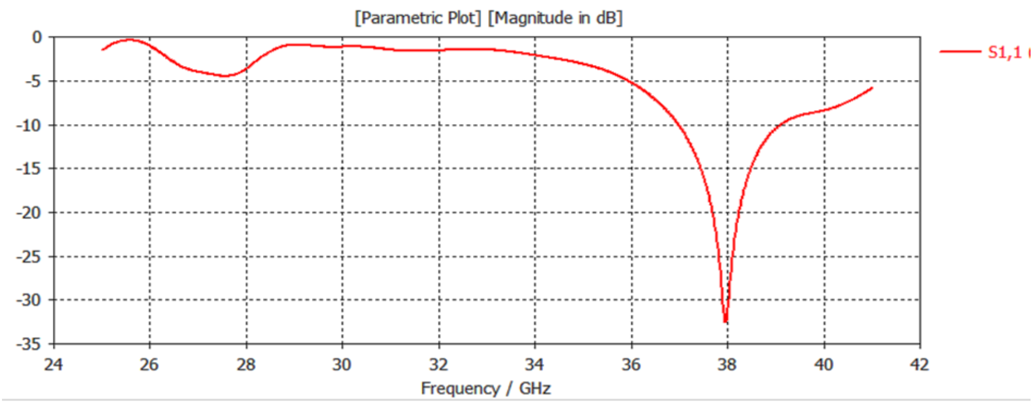

Fig. 6. Antenna reflection coefficient|S11| optimization for the proposed antenna at 38GHz.

It is noted that the return loss is less -10dB and it is ranging between 36.8 GHz and 40 GHz. Specifically, at 37.9 GHz the value of -34 dB has been observed from simulation. Moreover, the obtained bandwidth is 3 GHz. Fig. 7 shows the simulated radiation pattern of the proposed SIW slot antenna. It is noted that the maximum realized gain is equal to 6.66 dBi at 38 GHz. Furthermore, a side lobe level less than -10 dB and angular width (3 dB) equal to 115.9^{o} and 73.2^{o} are achieved in E-plane and H-plane respectively. The side lobe is a radiation lobe in any direction other than the main lobe. Moreover, a beam squint equal to 19^{o} at the E-plane and 1^{o} degree at the H-plane is observed. The proposed design exhibits an acceptable margin based on the cross polar pattern.

3.2. Step (II): Design of Single Band Slotted SIW Antenna at 28 GHz

In this step, the proposed antenna in step (I) is modified at 28 GHz and shown in Fig. 8. The coupling slots are cut on the top surface of the SIW but with different dimensions. As mentioned in step (I), SIW slotted antenna has longitudinal slots in the upper metallic layer of the waveguide and parallel to the length of the guide. As shown in Fig. 8, the longitudinal top wall slot in a SIW operates as a resonant mode with a resonant length of approximately λg/2. The closest short circuit is located about $\lambda_g/4$ or $3\lambda_g/4$ away from the center of the slot, Y_{slot}. These slots cut transverse shunt currents along the longitudinal direction of the SIW's top wall. For 28 GHz single band operation, both the lengths and widths of ***slot1*** and ***slot2*** are 3.9 mm and 0.4 mm, respectively. The design parameters values are optimized and listed in Table 2.

Table 2. The optimized parameters of designed antenna at 28 GHz.

Symbol	Value (mm)	Description
W	7	Antenna width
L	26.5	Antenna length
P	1	Center-to-center via holes separation
D	0.5	via holes diameter
A	5.5	Waveguide width
L_{s1}	3.9	Length of slot1
H	0.254	Substrate thickness
h_{pec}	0.0175	Metal thickness
L_{s2}	3.9	Length of slot2
W_{s1}	0.4	Width of slot1
W_{s2}	0.4	Width of slot2
W_t	3	Tapered Transition width
L_t	3.5	Tapered Transition length
W_m	0.789	50Ω feed line width
L_{ms}	3	50Ω feed line length
X_{s1}	0.06	Position of slot1 at X-axis
X_{s2}	-1.15	Position of slot2 at X-axis
Y_{s1}	13.7	Position of slot1 at Y-axis
Y_{s2}	5	Position of slot2 at Y-axis

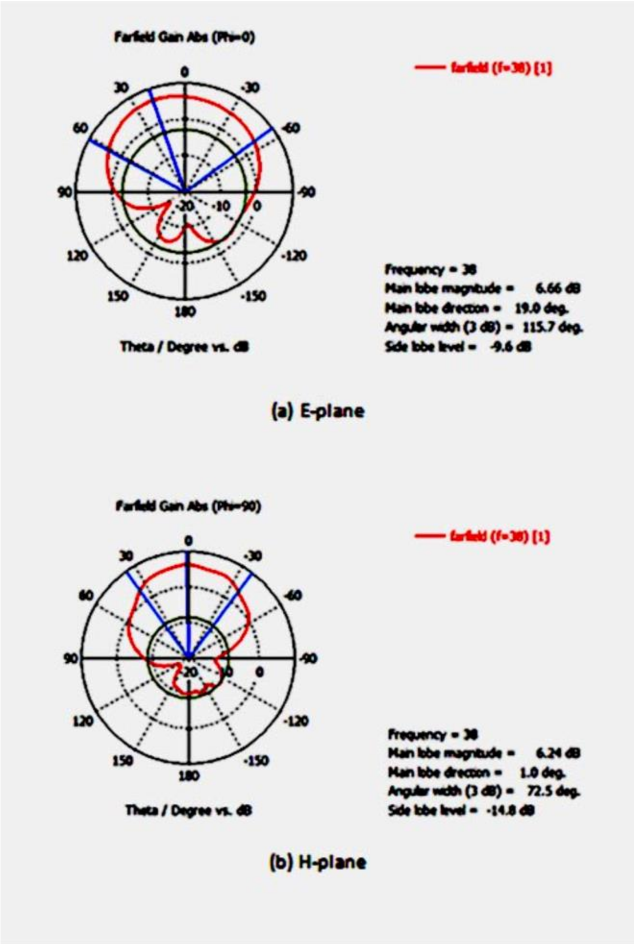

Fig. 7. E-Plane, H-Plane radiation pattern for SIW slotted antenna at 38GHz.

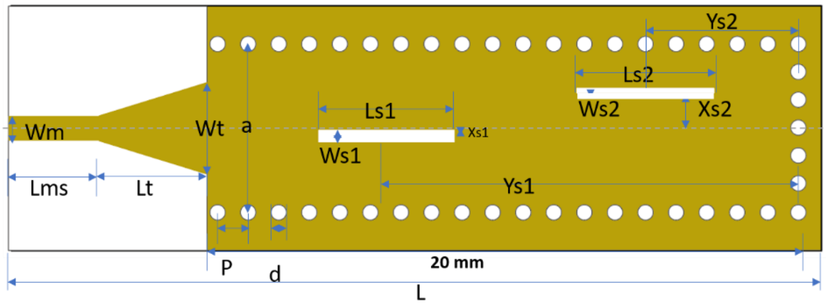

Fig. 8. SIW Dual-Slots Single Band Antenna at 28 GHz, Step (II).

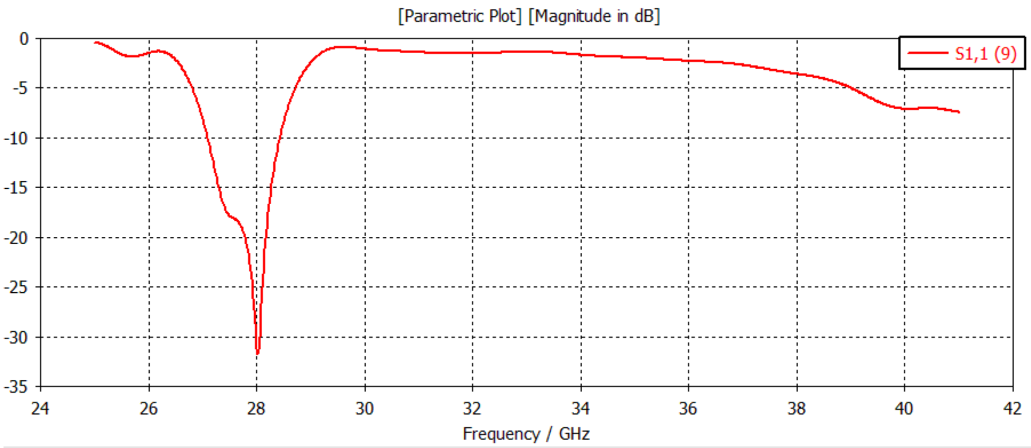

Fig. 9. Antenna reflection coefficient |S11| optimization for the proposed antenna at 28 GHz.

Fig. 9 shows the return loss |S11| of the proposed SIW slot antenna from 25 GHz to 40 GHz. It is observed that the return loss is below -10dB and ranging between 27.13 GHz and 28.45 GHz, and -32 at 28 GHz exactly. Bandwidth of 1.34 GHz is achieved. The simulated radiation pattern of the SIW slot antenna at 28 GHz is shown in Fig.10. It is observed that the maximum realized gain is equal to 6.35 dBi at 28 GHz. Furthermore, a side lobe level less than -10 dB and angular width (3 dB) equal to 96.7^o in E-plane and 80^o in H-plane are achieved. Furthermore, the radiation pattern exhibits a beam squint of 19 degrees in the E-plane and 9 degrees in the H-plane. The cross-polarization pattern indicates that the proposed design has an acceptable margin.

3.3. Step (III): 28/38 GHz Dual Band Antenna Design

The dual-frequency two-slot antenna designed shown in Fig. 11 is based on the theoretical calculation of the resonance frequencies of the TE_{10} mode of the SIW resonator, as described by equations (1) and (2). The antenna design also incorporates a tapered microstrip line transition due to its wide bandwidth characteristics. It is worth noting that the resonance frequencies and frequency differences of the dual-frequency two-slot antenna can be adjusted by modifying various parameters such as the equivalent length of the substrate, the length and width of the slots, and the position of the slots in the SIW structure. The dimension of the transition and the dimension of both slots with their positions after being optimized are shown in Table 3. The resonance frequencies of 28 and 38 GHz are affected by varying of the slots position length on SIW, which makes the frequencies of the antenna adjustable. Fig.12. shows the simulated results of input reflection coefficients (|S11|) of the proposed antenna which resonances at 28 GHz and 38 GHz before optimizing of antenna parameters. On the other hand, Fig.13. shows the simulated results of input reflection coefficients (|S11|) of the proposed antenna which resonances at 28 GHz and 38 GHz after optimizing of antenna parameters.

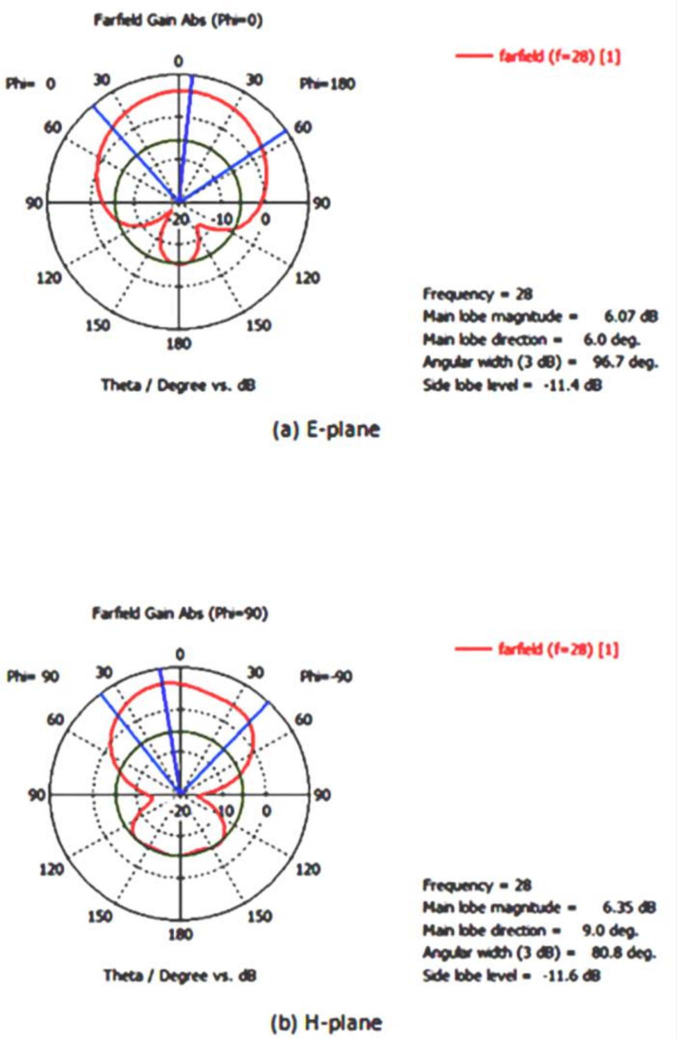

Fig. 10. E-Plane, H-Plane radiation pattern for SIW slotted antenna at 28GHz.

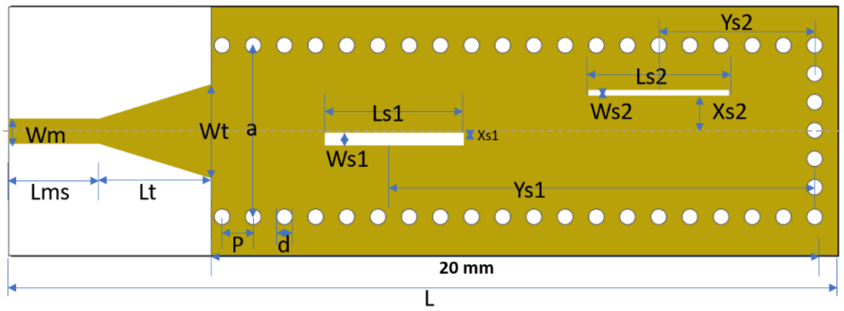

Fig. 11. The proposed SIW slots dual-band antenna.

Table 3. Antenna design parameters for 28/38 GHz (Phase-III)

Symbol	Value (mm)	Description
W	7	Antenna width
L	26.5	Antenna length
P	1	Center-to-center via holes separation
D	0.5	via holes diameter
A	5.5	Waveguide width
L_{s1}	4.5	Length of slot1
H	0.254	Substrate thickness
h_{pec}	0.0175	Metal thickness
L_{s2}	4.45	Length of slot2
W_{s1}	0.4	Width of slot1
W_{s2}	0.17	Width of slot2
W_t	3	Tapered Transition width
L_t	3.5	Tapered Transition length
L_{ms}	3	50Ω feed line length
W_m	0.789	50Ω feed line width
X_{s1}	0.06	Position of slot1 at X-axis
X_{s2}	-1.15	Position of slot2 at X-axis
Y_{s1}	13.48	Position of slot1 at Y-axis
Y_{s2}	5	Position of slot2 at Y-axis

Fig. 13 shows the return loss |S11| of the proposed SIW slot antenna with various dimensions. It is observed that for the dimensions shown in Table 3 about the optimal dimensions that describe the behavior of the curve, the return loss of the dual-frequency two-slot antenna varies between 27.1 and 28.4 GHz in the 28 GHz band, and between 36.8 and 40 GHz in the 38 GHz band. In addition, it is observed that the return losses are lower than -32 dB for band 28 GHz and lower than -38 dB for frequency band 38 GHz. Finally, Figs 14 and 15 show the simulated radiation pattern including both co-polarization and cross-polarization of the designed dual band antenna. It is noted that the maximum realized gain with values of 6.1 dBi and 5.81 dBi are obtained at 28 GHz and 38 GHz respectively. Angular width (3 dB) is 97^{o} in E-plane and 80^{o} degree in H-plane are achieved at 28 GHz, and at 38 GHz is 115^{o} in E-plane and 73^{o} in H-plane.

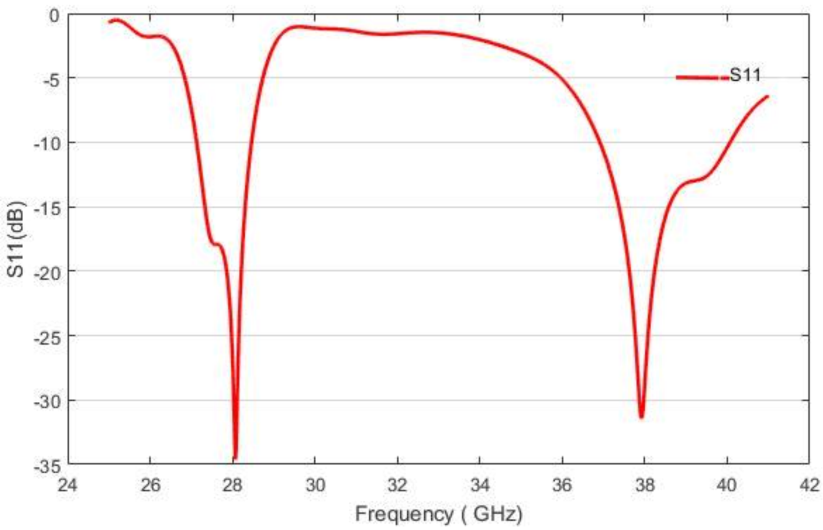

Fig. 12. Antenna reflection coefficient |S11| for the proposed antenna before parameters optimizing

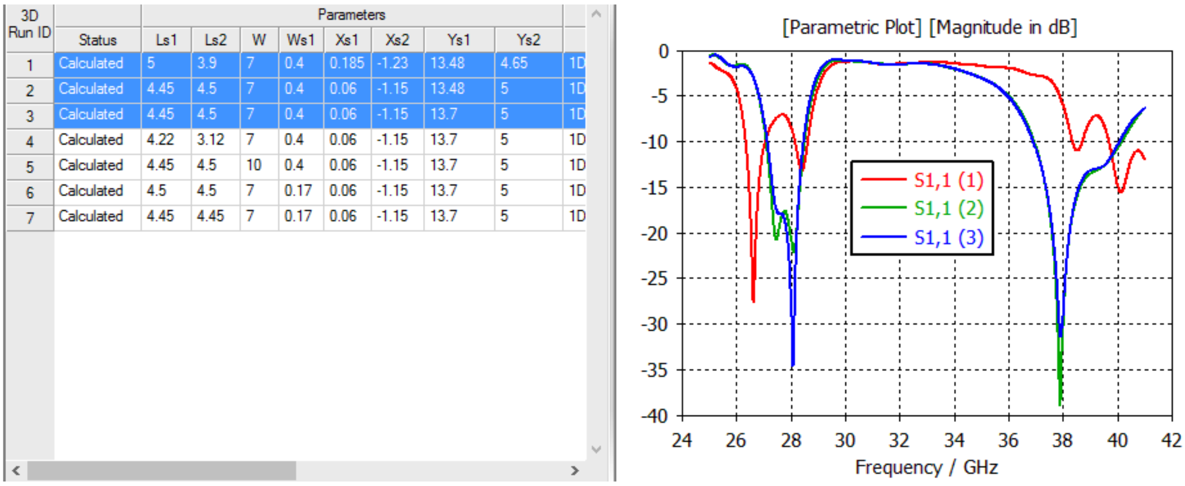

Fig. 13. Antenna reflection coefficient |S11| for the proposed antenna after parameters optimizing.

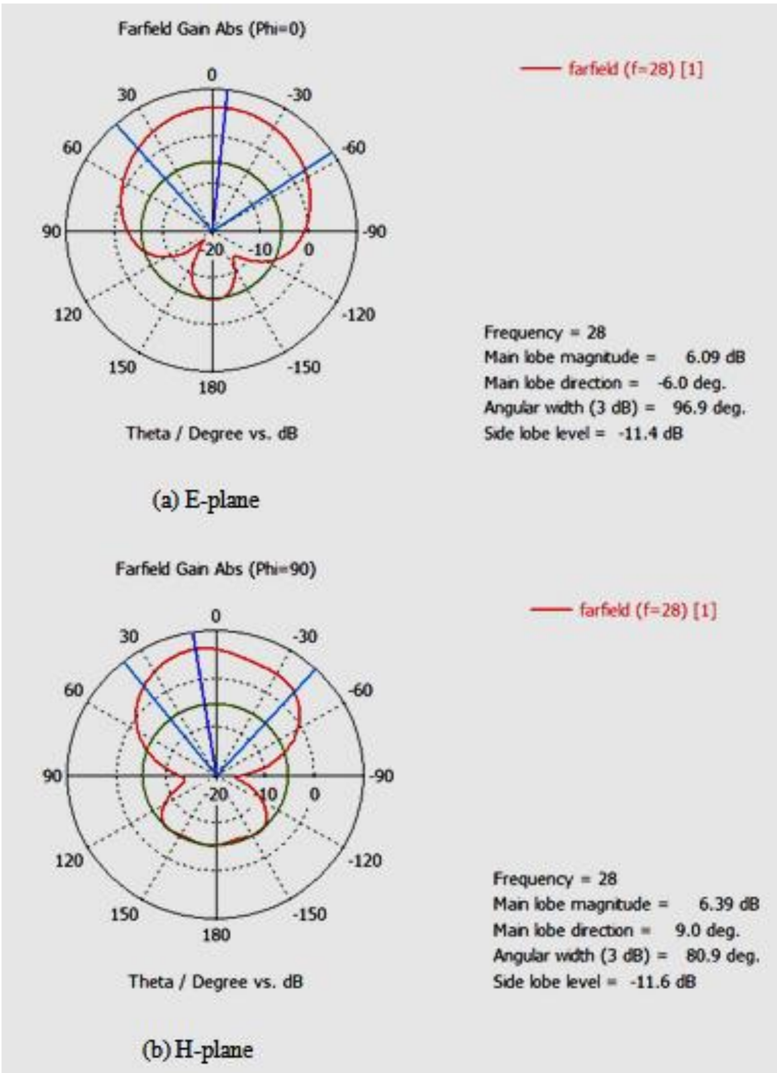

Fig. 14. H-Plane, E-Plane radiation pattern for SIW slotted antenna at 28GHz.

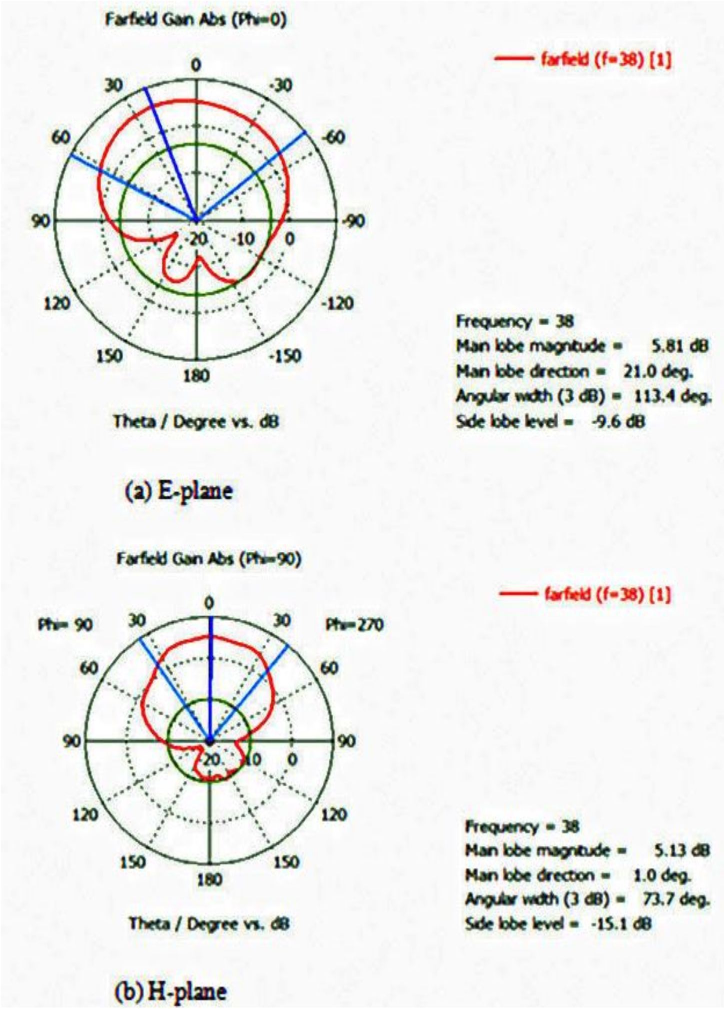

Fig. 15. E-Plane, H-Plane radiation pattern for SIW slotted antenna at 38GHz.

4. Comparison with Previous Works at 28 GHz and 38 GHz

Finally, Table 4 presents a comparison of the proposed dual-frequency two-slot antenna's performance with that of referenced antennas in terms of bandwidth, antenna size, return loss, and gain. The proposed antenna has a performance with excellent characteristics. The return loss of the proposed work is better than the other antennas of references mentioned in the table. Although the proposed antennas presented in [18. 23, 24] have quite larger gain than the proposed antenna, their antenna size is larger than our presented design. The antenna designed in [14] is the most relevant work. However, it differs from our work by the dimensions and a horizontally polarized linear array of four elements (1 × 4) was designed. In our work, two elements (1×2) were used. Furthermore, the performance of the proposed antenna in our work is better than that work as mentioned in Table 4. Therefore, the proposed antenna can satisfy the stringent demands of future wireless communication systems.

Table 4. The proposed antenna Comparison and other published works

Reference No	Resonant Frequency	Bandwidth (GHz)	Antenna Size (mm^3)	Return Loss	Gain (dBi)
[14]	28,38	0.45, 2.20	>26×5.5×0.254	-25, -23	5.2, 5.9
[18]	28, 38	0.98, 0.35	N/A	-17.3, -34.39	7.05, 8.32
[22]	28,38	2.83, 7.92	6×8×0.254	N/A	N/A
[23]	28.044, 38.04	N/A	55×110×0.505	-21.57, -24.59	7.95, 8.25
[24]	28, 38	0.9, 0.4	30×7.50×0.254	-16, -29	7.2, 11.2
[25]	28, 38	1.43, 3.54	8×8×8	-10, -20	2.7, 6
[26]	28, 38	1.49, 1.01	13×11.25×2.2	-23.6, -27.1	5.41, 4.89
[27]	28/38	2.55, 2.1	26×14×0.38	-35, -36	1.27, 1.83 (peak gain)
[28]	28,38	1.23, 1.06	7.5 ×8.8 ×0.25	-34.5, -27.3	6.6, 5.86
[29]	28/38	1.39 3.33	41.5 ×10 ×0.8	N/A	5.7
This work	28, 38	1.32, 3.16	26.5×7×0.254	<-38, -32	6.39, 5.13

5. Conclusion

In this paper, a $20\times7\times0.254mm^3$ a dual band antenna millimeter wave has been proposed for future cellular communication systems using SIW. The proposed antenna operates at a dual band of 28/38 GHz, which is appropriate for future wireless communication applications as decided by FCC. A low loss/cost substrate, RT/Duroid 5880 material, and a tapered microstrip line transition have been used in all prototypes. CST Microwave Studio software has been used to carry out all the results. The proposed antenna's parameters, such as the length and width of each slot and its positioning, as well as the substrate's thickness, were optimized and fine-tuned to achieve improved return loss, bandwidth, and efficiency. The gain of 6.1 dBi and 5.81 dBi at 28 GHz and 38 GHz have been obtained. A Bandwidth of 1.32 GHz and 3.1 GHz for 28 GHz and 38 GHz has been achieved respectively. The obtained results shown that the designed antenna achieves stable and tunable dual-frequency performance which makes it suitable to operate in the applications of various future wireless communication systems. Investigating the feasibility and practicality of implementing the proposed scheme through fabrication could be a fascinating avenue for future research.

References

[1] Access, E. U. T. R. Base station (bs) radio transmission and reception, 3gpp ts 36.104. V14 3 (2009).
[2] Commission, F. C. et al. Spectrum frontiers report and order and further notice of proposed rulemaking: Fcc16-89 (2016).
[3] K. Wu, "Integration and interconnect techniques of planar and non-planar structures for microwave and millimeter-wave circuits -current status and future trend," APMC 2001. 2001 Asia-Pacific Microwave Conference (Cat. No.01TH8577), Taipei, Taiwan, 2001, pp. 411-416 vol.2, doi: 10.1109/APMC.2001.985398.
[4] K. Wu, Y. J. Cheng, T. Djerafi and W. Hong, "Substrate-Integrated Millimeter-Wave and Terahertz Antenna Technology," in Proceedings of the IEEE, vol. 100, no. 7, pp. 2219-2232, July 2012, doi: 10.1109/JPROC.2012.2190252.
[5] K. Wu, M. Bozzi and N. J. G. Fonseca, "Substrate Integrated Transmission Lines: Review and Applications," in IEEE Journal of Microwaves, vol. 1, no. 1, pp. 345-363, Jan. 2021, doi: 10.1109/JMW.2020.3034379.
[6] A. Dahiya and D. Deshwal, "Design Fundamentals: Iris Waveguide Filters Versus Substrate Integrated Waveguide (SIW) Bandpass Filters," in Proceedings of International Conference on Artificial Intelligence and Applications, Singapore: Springer Singapore, 2021, pp. 195–202. https://doi.org/10.1007/978-981-15-4992-2_19
[7] A. Dahiya, R. Anand, N. Sindhwani, and D. Deshwal, "Design and construction of a low loss substrate integrated waveguide (SIW) for S band and C band applications," Mapan, vol. 36, no. 2, pp. 355–363, 2021. https://doi.org/10.1007/s12647-021-00449-x
[8] T. Deckmyn, M. Cauwe, D. Vande Ginste, H. Rogier and S. Agneessens, "Dual-Band (28,38) GHz Coupled Quarter-Mode Substrate-Integrated Waveguide Antenna Array for Next-Generation Wireless Systems," in IEEE Transactions on Antennas and Propagation, vol. 67, no. 4, pp. 2405-2412, April 2019, doi: 10.1109/TAP.2019.2894325.
[9] N. Al-Fadhali, H. A. Majid, R. Omar, M. K. A. Rahim, S. M. Shah and B. A. F. Esmail, "Wideband (22-30GHz) mm-Wave Substrate Integrated Waveguide (SIW) Antenna for 5G Applications," 2019 IEEE Conference on Antenna Measurements & Applications (CAMA), Kuta, Bali, Indonesia, 2019, pp. 1-4, doi: 10.1109/CAMA47423.2019.8959544.
[10] P. Kumawat and S. Joshi, "Review of Slotted SIW antenna at 28 GHz and 38 GHz for mm-wave applications," 2020 12th International Conference on Computational Intelligence and Communication Networks (CICN), Bhimtal, India, 2020, pp. 8-13, doi: 10.1109/CICN49253.2020.9242587.
[11] M. A. Matin, "Review on millimeter wave antennas- potential candidate for 5G enabled applications," Adv. Electromagn., vol. 5, no. 3, p. 98, 2016.
[12] G. A. Casula, G. Mazzarella, G. Montisci, and G. Muntoni, "A review on improved design techniques for high performance planar waveguide slot arrays," Electronics (Basel), vol. 10, no. 11, p. 1311, 2021, https://doi.org/10.3390/electronics10111311
[13] P. Kumawat and S. Joshi, "5G dual-band slotted SIW array antenna," J. Taibah Univ. SCI, vol. 15, no. 1, pp. 321–328, 2021. https://doi.org/10.1080/16583655.2021.1978830
[14] N. Ashraf, O. Haraz, M. A. Ashraf and S. Alshebeili, "28/38-GHz dual-band millimeter wave SIW array antenna with EBG structures for 5G applications," 2015 International Conference on Information and Communication Technology Research (ICTRC), Abu Dhabi, United Arab Emirates, 2015, pp. 5-8, doi: 10.1109/ICTRC.2015.7156407.
[15] W. Y. Yong, A. Haddadi, T. Emanuelsson and A. A. Glazunov, "A Bandwidth-Enhanced Cavity-Backed Slot Array Antenna for mmWave Fixed-Beam Applications," in IEEE Antennas and Wireless Propagation Letters, vol. 19, no. 11, pp. 1924-1928, Nov. 2020, doi: 10.1109/LAWP.2020.3022988.
[16] H. -N. Hu, F. -P. Lai and Y. -S. Chen, "Dual-Band Dual-Polarized Scalable Antenna Subarray for Compact Millimeter-Wave 5G Base Stations," in IEEE Access, vol. 8, pp. 129180-129192, 2020, doi: 10.1109/ACCESS.2020.3009431.
[17] R. Y. Mianroodi, H. Aliakbarian and G. A. E. Vandenbosch, "Dual-port dual-band (28/38 GHz) SIW leaky wave antenna for 5G base stations," 12th European Conference on Antennas and Propagation (EuCAP 2018), London, UK, 2018, pp. 1-4, doi: 10.1049/cp.2018.1212.
[18] J. Singh, F. Lal Lohar, and B. S. Sohi, "Design of dual band millimeter wave antenna using SIW material for 5G cellular network applications," Mater. Today, vol. 45, pp. 5405–5409, 2021. https://doi.org/10.1016/j.matpr.2021.02.106
[19] Djerafi, T., Doghri, A., Wu, K.. Substrate Integrated Waveguide Antennas. In: Chen, Z. (eds) Handbook of Antenna Technologies. Springer, Singapore, 2015. https://doi.org/10.1007/978-981-4560-75-7_57-1
[20] krn: "CST Studio Suite 3D EM simulation and analysis software," https://www.3ds.com/products-services/simulia/products/cst-studio-suite/?utm_source=cst.com&utm_medium=301&utm_campaign=cst, accessed May 2022.
[21] F. Alnemr, M. F. Ahmed, and A. A. Shaalan, "A compact 28/38 GHz MIMO circularly polarized antenna for 5 G applications," J. Infrared Millim. Terahertz Waves, vol. 42, no. 3, pp. 338–355, 2021. https://doi.org/10.1007/s10762-021-00770-1

[22] H. Ullah, F. A. Tahir and Z. Ahmad, "A Dual-band Hexagon Monopole Antenna for 28 and 38 GHz Millimeter-Wave Communications," 2018 IEEE International Symposium on Antennas and Propagation & USNC/URSI National Radio Science Meeting, Boston, MA, USA, 2018, pp. 1215-1216, doi: 10.1109/APUSNCURSINRSM.2018.8608274.

[23] Marzouk, H.M., Ahmed, M.I., Shaalan, A.-E.H.: "Novel dual-band 28/38 GHz Mimo antennas for 5g mobile applications" Progress In Electromagnetics Research. C Pier C., 2019, 93, pp. 103–117. doi:10.2528/PIERC19032303

[24] P. Kumawat and S. Joshi, "Design of 28/38 GHz Dual-Band SIW Slot antenna for 5G Applications," Int. J. Eng. Res. Technol. (Ahmedabad), vol. 8, no. 17, 2020. DOI : 10.17577/IJERTCONV8IS17005

[25] S. Muhammad, I. Ya'u, A. S. Abubakar, and A. S. Yaro, "Design of single feed dual-band millimeter wave antenna for future 5G wireless applications," Sci. World J., vol. 14, no. 1, pp. 84–87, 2019.

[26] Muhammad Anab Muhammad Irfan Khattak Syed Muhammad Owais Abbas Ali Khattak Asif Sultan, "Design and Analysis of Millimeter Wave Dielectric Resonator Antenna for 5G Wireless Communication Systems," Progress In Electromagnetics Research C, Vol. 98, 239-255, 2020. doi:10.2528/PIERC19102404.

[27] M. N. Hasan, S. Bashir, and S. Chu, "Dual band omnidirectional millimeter wave antenna for 5G communications," J. Electromagn. Waves Appl., vol. 33, no. 12, pp. 1581–1590, 2019. https://doi.org/10.1080/09205071.2019.1617790

[28] A. E. Farahat and K. F. A. Hussein, "Dual-Band (28/38 GHz) Wideband MIMO Antenna for 5G Mobile Applications," in IEEE Access, vol. 10, pp. 32213-32223, 2022, doi: 10.1109/ACCESS.2022.3160724.

[29] Umair Rafique, Shobit Agarwal, Nasir Nauman, Hisham Khaliland Khalil Ullah , "Inset-Fed Planar Antenna Array for Dual-Band 5G MIMO Applications," Progress In Electromagnetics Research C, Vol. 112, 83-98, 2021. doi:10.2528/PIERC21021302.

Authors' Profiles

Khaled A. M. Al Soufy has received his B.Sc in Computer and control engineering from Sana'a University, Yemen, in 1998 and his M.Tech in Computer Science and Engineering from Osmania University, Hyderabad, India in 2006. He received his Ph.D. (2012) in Computer Engineering, from department of computer Engineering, Z.H. College of Engineering and Technology, Aligarh Muslim University, Aligarh, India. He has joined the teaching staff of the Department of Electrical Engineering, Faculty of Engineering, Ibb University, Yemen, in 2013. He is currently an Associate Professor with the Department of Electrical Engineering at Ibb University, Yemen. He worked as a head of the Electrical Engineering Department in the Faculty of Engineering of the University of Ibb from 2014-2018 and as a Vice Dean of the Students Affairs of the Faculty of Engineering at the University of Ibb from 2018-2021. Since October 2021, he has been a visiting scholar in the School of Engineering and Science at the American University in Cairo, Egypt. His research interest includes mobile computing and Quality of service in mobile computing, Sensor network, wireless network, image and signal processing, Machine Learning. He has more than 20 research publications

Nagi H. Al-Ashwal has a B.Sc. in Electrical Engineering from Sana'a University, Sana'a, Yemen (1997), a M.Sc. (2003) and Ph.D. (208) in Computer Engineering from Assiut University, Egypt. He joined the Electrical Engineering Department, at the University of Ibb, Ibb, Yemen in 2018 as an Assistant Professor and became Associate Professor in November 2013. Since September 2021, he has been a visiting scholar in the School of Electrical of the Engineering and Science in the American University in Cairo, Egypt. He worked as a head of the Electrical Engineering Department in the Faculty of Engineering of the University of Ibb from 2009-2011 and as a Dean of the Faculty of Engineering at the University of Ibb from 2015-2021. His research interests are Computer Vision, Image processing and pattern recognition. He has many publications in these fields.

Faisal Al-Kamali has a B.Sc. in Electronics and Communication Engineering from the University of Baghdad, Baghdad, Iraq (2001), a M.Sc. (2008) and Ph.D. (2011) in Communication Engineering from the University of Minufia, Egypt. He joined the Electrical Engineering Department, at the University of Ibb, Ibb, Yemen in 2011 as an Assistant Professor and became Associate Professor in January 2017. Since November 2021, he has been a visiting scholar in the School of Electrical Engineering and Computer Science in the Faculty of Engineering at the University of Ottawa, Canada. He worked as a head of the Electrical Engineering Department in the Faculty of Engineering of the University of Ibb from 2013-2014 and as a Vice Dean of the Academic Affairs of the Faculty of Engineering at the University of Ibb from 2018-2020. His research interests are in physical layer technologies for wireless communication systems such as interference cancellation, channel equalization and channel estimation, image transmission over wireless communication systems, hybrid precoding and combining, mmWave systems, and massive MIMO systems. Faisal Al-Kamali was a recipient of the prize of supervising the best graduation project in Ibb University in 2016.

Redhwan M. A. Saad obtained his Ph.D in Internet Infrastructure Security from University Sains Malaysia (USM). He is a senior lecturer at Electrical Department, Faculty of Engineering, Ibb University, Yemen. Currently he is a postdoctoral research fellow at Computer Engineering department, Cairo University. His current research interests include Cybersecurity, Internet of Things security, Intrusion Detection System (IDS), Intrusion Prevention System (IPS), and IPv6 security.

Majed A. AL-Sayadi has received his BSc in communication Engineering from Ibb University, Yeme, Currently, he is working at department of planning and optimization network at YEMENi OMANI TELECOMMUNICATIONS UNITED company. His interested research is wireless communication systems, signal processing.

How to cite this paper: Khaled A. M. Al Soufy, Nagi H. Al-Ashwal, Faisal S. Al-Kamali, Redhwan Saad, Majed A. AL-Sayadi, "Design of 28/38-GHz Dual-Band Millimeter Wave Antenna based on SIW for Future Cellular Communication Systems", International Journal of Wireless and Microwave Technologies(IJWMT), Vol.13, No.5, pp. 34-47, 2023. DOI:10.5815/ijwmt.2023.05.04